Contents lists available at ScienceDirect

Mechanical Systems and Signal Processing

journal homepage: www.elsevier.com/locate/ymssp

Continuous wavelet analysis of mode shapes differences for damage detection

Mario Solís, Mario Algaba, Pedro Galvín *

Escuela Técnica Superior de Ingeniería, Universidad de Sevilla, Camino de los Descubrimientos, 41092 Sevilla, Spain

ARTICLE INFO

ABSTRACT

This paper presents a new damage detection methodology for beams. It applies wavelet analysis to locate the damage from changes in the mode shapes (geometric based analysis). The proposed methodology requires the mode shapes of a reference undamaged state as well as those of the potentially damaged one. Once obtained, a continuous wavelet transform is applied to the difference of the mode shape vectors to obtain information of the changes in each of them. Finally, the results for each mode are added up to compute an overall result along the structure. For the addition, the wavelet coefficients of each mode are weighted according to the corresponding variation of the natural frequency. By doing so, emphasis is given on those modes that are more likely to be affected by damage. On the other hand, mode shapes that have not changed their natural frequencies are disregarded. The proposed methodology also includes mathematical techniques to avoid wavelet transform edge effect, experimental noise reduction in mode shapes and creation of new virtual measuring points. It has been validated by experimental analysis of steel beams with cracks of different sizes and at different locations. The results show that the method is sensitive to little damage. The paper analyses the severity threshold of damage and the required number of sensors to obtain successful results.

© 2013 Elsevier Ltd. All rights reserved.

1. Introduction

Vibration based Structural Health Monitoring (SHM) became an interesting research topic in structural mechanics around 30 years ago [1,2]. It is based on the fact that the loss of stiffness due to damage affects the dynamic response of the structure. Therefore, damage can be detected by monitoring and identifying the dynamic properties of a structure. Those parameters are mainly modal parameters such as natural frequencies, mode shapes and damping ratios.

Vibration based SHM is mainly attractive because of its ability to monitor and detect damage from a global testing of the structure. Thus, vibration based SHM is especially advantageous when compared with traditional SHM based on non-destructive testing methods (X-ray, Eddy-current examination, thermography, acoustic or ultrasonic waves, etc.), which require accessibility and measuring at any potentially damaged area.

In order to detect changes in the response of the structure induced by damage, the wavelet transform is a promising mathematical tool. Although wavelet transform background comes from the beginning of last century [3], its development as an engineering signal analysis tool is rather new. Wavelet transform is mainly attractive because of its ability to compress and encode information, to reduce noise, or to detect any local singular behavior of a signal. It is considered that the

---

pioneering application of wavelet transform to SHM was published in 1994 [4]. Since then, wavelet transform applications to damage detection have been developed by many authors [5,6]. For instance, Ren and Sun [7] defined the so-called wavelet entropy parameter, based on the Shanon entropy, as an efficient tool to detect changes in the time response of a structure. They could detect change in the natural frequencies and also the time when this change occurred. Sohn et al. [8] analyzed the time response of structures monitored with piezoelectric sensors and Deng et al. [9] studied the transient response of a steel beam and a composite panel due to an impact load to detect damage. For buildings, Yan et al. [10] defined a damage detection parameter from the accelerations of a rather large amount of sensors, and they could also detect the time when the damage appeared.

Wavelet transform is not only applied to time signals but also to space defined signals. When using a space based wavelet analysis, static deflection or mode shapes of the structure can be used [5,6]. It can be applied to one dimensional (beams) as well as two dimensional analysis (plates) [5,11]. Initially, Liew and Wang [12] and Wang and Deng [13] analyzed static deflections of beams for damage detection. After that, there have been numerical and experimental validations and analysis of multiple load situations [14–19]. When using multiple load situations, the displacements [18] or their difference to a reference state [19] may be combined to obtain an overall information of the structure.

If a modal analysis is performed, then wavelet analysis can be applied to mode shape vectors or their derivatives to detect changes induced by damage [11,20–30]. It has been successfully applied to beams made of aluminum [21], wood [22] or plexiglass [11]. Zhong and Oyadiji [21,23] proposed a methodology for damage detection in beams based on the difference of wavelet coefficients of each half of the beam. They analyzed the effect of the sampling distance, and they introduced a spline interpolation to increase the number of input points for the wavelet transform. They also proposed a damage parameter based on the addition of the results for all the mode shapes. Gokdag and Kopmaz [26] proposed another methodology that obtains the information of the undamaged state from the damaged mode shapes, so a preliminary test of the undamaged structure is not required. The undamaged mode shapes are approached from the approximation coefficients of a Discrete Wavelet Analysis of the damaged mode shapes. Recently, Radziensky et al. [27] proposed a hybrid damage detection method for beams. They employed the change in natural frequencies and modal curvatures to define a damage probability function which was used to weight the wavelet coefficients along the beam for each mode shape, and eventually results for each mode shape were added up. There are also papers devoted to analyze the effect of not only crack positions but crack depth and the effect of multiple cracks [24,25,28].

In this paper, a new wavelet based damage detection method is proposed in which modal parameters and wavelet analysis are combined. It is based on the analysis and addition of the coefficients of the continuous wavelet transform of the difference of mode shapes between an undamaged and a damaged state. For the addition, changes in natural frequencies are used to weight the difference in mode shapes. The wavelet coefficients obtained for each mode shape, as well as the addition for all the mode shapes are used as damage detection parameters. This paper deals with modal testing of steel beams for which the presence and location of damage is analyzed. This kind of testing could be applied to quality control and health monitoring of any beam like structural element. However, it could be extended to beam like civil structures or any structure which can be considered to be one dimensional for monitoring and for which any information about the behavior of the cross section is not needed. Such kind of structures could be bridges [31], masts [32], slender buildings, etc.

The paper is organized as follows. Firstly, the paper reviews the definition of the wavelet transform, as well as some of its mathematical properties and requirements. Then, the proposed methodology is described, and the results that have been obtained for steel beams with cracks of different size and located at different positions are presented. Finally, conclusions are drawn.

2. Wavelet transform

This section presents some basic ideas and definitions about wavelet transform. It is focused on the understanding of wavelet transform meaning, application and utility. It is not aimed at giving an exhaustive and rigorous mathematical review of the wavelet transform, so it will consider only some basic concepts and definitions. Further fundamental explanations can be found elsewhere (e.g. [33]). Firstly, the wavelet transform is compared to the well known Fourier transform in order to illustrate some of its main features and provide an easy understanding of its meaning. Then, some mathematical definitions and properties of wavelet analysis are introduced.

2.1. Fourier and wavelet transforms

A linear transformation of function $f(t)$ can be defined as

$$T = \int_{-\infty}^{\infty} \phi(t) \cdot f(t)\, dt \tag{1}$$

The resulting function T shows how similar is the original function to the integration function $\phi(t)$. For a Fourier transformation, function $\phi(t)$ is a stationary harmonic function of type $e^{i\omega t}$, where ω is the harmonic frequency. Thus, the resulting function T depends only on ω and it only gives information about the harmonic frequency content of the overall original signal. Fourier transform does not retain any time information of the signal, such as the time evolution of its frequency content.

In order to obtain some time information about the frequency content, one may apply a Short Time Fourier Transform (STFT). In that case, the harmonic transforming function would be affected by a window function $w(t-\tau)$ that could be a rectangular, exponential of any window function that is null out of the window interval. Therefore, it is considered only a certain part of the original signal for each value of τ. By translation of the window function (modifying parameter τ), the original signal is divided into windows and a Fourier transform is applied to each window. Therefore, some time information is obtained from the time windowing and the resulting transformed function T not only depends on ω but also on the convolution parameter τ.

When using the wavelet transform, function ϕ is a wavelet family defined through translation and dilatation of a function $\Psi(t)$:

$$\phi_{u,s}(t) = \frac{1}{\sqrt{s}} \Psi\left(\frac{t-u}{s}\right) \tag{2}$$

Parameter u is known as the translation parameter and u/s is equivalent to the STFT convolution parameter τ. Parameter s is defined as the scale of the wavelet transform. It defines the shrinking or stretching of the wavelet function and $1/s$ plays an equivalent role to Fourier frequency ω. The resulting wavelet transformed function T will depend on scale s and translation parameter u. Function T will indicate how similar the original function is to the wavelet function for a specific location, given by the value of the translation parameter, and for a specific scale.

The inverse of s can be interpreted as a pseudo-frequency, since it modulates the frequency content of the wavelet function, but the wavelet function is not a harmonic function itself. Higher scales corresponds to lower frequencies and vice versa. A value of the corresponding pseudo-frequency for each scale can be obtained from the following expression [34,35]:

$$F_a = \frac{F_c \cdot f_s}{a} \tag{3}$$

where F_a is the pseudo-frequency for scale a, f_s is the sampling frequency, and F_c is the center frequency of the wavelet. F_c can be interpreted either as the frequency that gives a maximum of the Fourier transform of the wavelet function, or the frequency of a harmonic function that maximizes the wavelet transform coefficients. Thus, a harmonic function of a frequency equal to the center frequency captures the main wavelet oscillations (Fig. 1). The center frequency is a convenient and simple characterization of the dominant frequency of the wavelet.

Therefore, the wavelet transform gives time information of the frequency content of the signal, whereas no time information is obtained with Fourier analysis and certain time information is obtained with STFT. On the other hand, the wavelet analysis can provide higher time resolution for higher frequencies and lower time resolution for lower frequencies, since the convolution parameter (u/s) can be adapted according to frequency.

The previous analysis based on time and frequency can be identically applied in terms of a linear geometric coordinate and geometric frequency. Thus, t, τ and u could be referred to a geometric dimension. In that case, the transformation gives information about the spatial evolution of the original function. In this paper, the wavelet transform is applied to signals (mode shapes) defined along a geometric coordinate (position along a beam).

2.2. Continuous wavelet transform background

In order to be a good candidate for wavelet analysis, a wavelet family should fulfill several mathematical requirements, although not all of them are mandatory for every application.
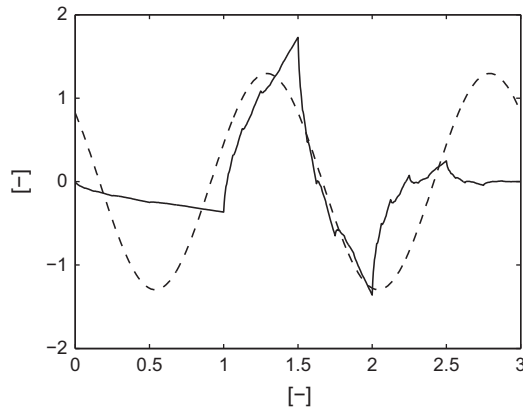

Fig. 1. Wavelet function Daubechies type with two vanishing moments (solid line) and its associated center frequency based approximation (dashed line).

The wavelet function Ψ is an oscillatory function that must have a zero average and finite length, that is, compact support:

$$\int_{-\infty}^{+\infty} \Psi(x)\,dx = 0 \tag{4}$$

The stationary behavior of a harmonic function does not fulfill the compact support requirement.

Ψ is centered at $x=0$ and it also must fulfill the wavelet admissibility condition [36]:

$$\int_{0}^{+\infty} \frac{|\Psi(\omega)|^2}{\omega}\,d\omega < \infty \tag{5}$$

where $\Psi(\omega)$ is the Fourier transform of $\Psi(t)$.

The Continuous Wavelet Transform (CWT) of a function $f(t)$ can be defined as

$$CWT_f(u,s) = \frac{1}{\sqrt{s}} \int_{-\infty}^{+\infty} f(x)\Psi^*\left(\frac{x-u}{s}\right) dx \tag{6}$$

where Ψ^* indicates the complex conjugate of the wavelet function. $CWT_f(u,s)$ indicates the content of the scaled wavelet shape in the original function $f(x)$ at a specific location. This can be understood in the sense of time evolution of frequency content, as it was explained above.

As for the Fourier transform, there is a Discrete Wavelet Transform (DWT) for which discrete values of translation and scales are used. The DWT is more efficient than CWT for computation and signal encoding. Typically, the DWT is computed following a multi-resolution analysis [5,37], that gives an adaptive time (or space) – frequency (or scale) resolution. In that case, only coefficients for a certain discrete numbers of scales and translation parameters are obtained. When using the CWT, translation and scale parameters are continuous, giving more coefficients than necessary to strictly obtain the necessary information of the signal. For instance, more coefficients than needed to reconstruct the original signal. However, this redundancy provides a more clear information to detect changes or singularities in the original function, and therefore CWT is usually preferred for SHM applications.

An important feature of a wavelet function is its number of vanishing moments. If a wavelet function has N vanishing moments, then

$$\int_{-\infty}^{+\infty} x^k \Psi(x)\,dx = 0 \quad \text{for} \quad k = 0 \ldots N-1 \tag{7}$$

For any polynomial of smaller order than the number of vanishing moments, the wavelet transform will give null values. Therefore, the number of vanishing moments indicates how sensitive is the wavelet to low order signals, and it can be chosen so as to take only into account the components of the signal above certain order value.

The sensitivity of the wavelet transform to changes induced by damage depends on the wavelet family and the number of vanishing moments of the wavelet function. The choice of these parameters should be based on a mathematical analysis of the nature of the signal to be studied as well as the expected effect of damage [15,30]. However, this mathematical analysis is not always clear a priori and in most applications these parameters are chosen depending on previous results or on trial and error [5].

In this paper, the well-known Daubechies [36] wavelet family with 2 vanishing moments has been used. This number is considered as the minimum value for crack detection [30,38]. For the beams analyzed in this paper, a higher number of vanishing moments proved to be less sensitive to damage detection and location. That may suggest that the effect of damage induces a change of order 2 in mode shapes that should not be neglected. The next sections include some additional comments and results about the significance and influence of the number of vanishing moments.

3. Combined modal-wavelet methodology for damage detection

In this section, the proposed methodology for damage detection in beams is described step by step.

3.1. Modal analysis

The first task of the proposed methodology is to obtain the mode shapes and natural frequencies of the structure. As any vibration based damage detection method, it requires modal information about the undamaged and damaged state.

If the structure to be analyzed can be tested in laboratory conditions, an Experimental Modal Analysis (EMA) can be performed. A controlled and measured input force is applied to the structure and the dynamic response at certain measuring points are analyzed to obtain natural frequencies and mass normalized mode shapes [39]. If the structure is large and/or must keep under service loads (bridges, masts, etc.) then an Operational Modal Analysis (OMA) can be carried out [40,41]. In that case, the ambient excitation forces are unknown and scaled mode shapes are not obtained. If some exogenous controlled force is introduced, then a Combined Stochastic Subspace Identification (CSSI) can be applied and scaled mode shapes are obtained [42]. As it was stated at the first section of the paper, the proposed damage detection methodology could be applied to different kind of structures. Thus, the system identification method is not relevant for the

methodology proposed in the present paper, and the choice would depend on the specific application where it is used. The contribution of the paper is focused on how to deal with damage detection once the mode shapes and frequencies have been identified.

3.2. Extension of mode shapes

The next step of the methodology deals with a very important issue in wavelet analysis, especially when applied to space based damage detection. The wavelet transform is defined for an infinite integration interval, whereas the original signal is defined over a finite interval. When the wavelet transform is performed, there is a singular behavior at the beginning and at the end of the signal. The signal starts and finishes at those points, so there is a significant local change there, unless the signal trends softly in an asymptomatic way to a constant value, which will never be the case for a mode shape. This phenomenon is similar to the leakage effect in the Fourier transform, as it is due to the finite and non-stationary nature of the original signal, being inconsistent with the infinite integral of the Fourier transform.

This unstable behavior of the wavelet coefficients in the vicinity of the beginning and the end of the analyzed signal is known as the edge effect, and it is a serious drawback of the wavelet transform when the damage is close to the beginning or the end of the signal. Moreover, the high values of wavelet coefficients near those regions of the signal can mask the structural damage effect on the wavelet transform along the structure.

A detailed discussion about this issue can be found in the work of Messina [43]. He proposed some advanced methods to avoid the edge effect based on isomorphism and self-minimization applied to an extension of the original signal. An alternative and simplified methodology has been proposed by Rucka and Wilde [16], applying an extension of four points using a cubic spline. Previous works [20,44] also proposed the use of a window function to weight the wavelet coefficients, so the coefficients near the edges were reduced, but that implies that information is not reliable for these areas. This paper applies a simpler method to avoid edge effects. It consists of an antisymmetric extension of the signal of the same length of the original signal at both ends [33]. Fig. 2 illustrates the extension technique. The wavelet analysis will be performed on the extended signal so the edge effects will appear at the beginning and at the end of this signal. The interesting results will only be those related to the original signal, that will be free of edge effects.

3.3. Smoothing, interpolation and noise reduction of mode shapes

Another important issue when analyzing mode shapes is the reduction of experimental noise effect. The experimental mode shapes will always be affected by noise, so they will always show some kind of irregularities. This undesirable behavior will affect the wavelet analysis and it could eventually mask the effect of damage. In order to reduce this effect, a smoothing technique may be introduced, so local peaks induced by experimental noise are eliminated without affecting any local trend that could have been induced by damage, since damage is not expected to produce only a local peak as it is the case of experimental noise. The softening technique proposed in this paper uses 'mslowess' built-in function of Matlab software [35]. It is applied using a weighted quadratic least squares approach performed at every location of the original mode shape considering a span including ten neighboring points centred at that location. The regression weights for each data point in the span are given by the following cubic function:

$$W_i = \left(1 - \left(\frac{x-x_i}{dx}\right)^3\right)^3 \quad i = 1,..10 \tag{8}$$

where W_i is the weight for point i in the considered span, x is the location of the point to be smoothed, x_i is the location of point i and dx is the physical length of the span. Fig. 3(a)–(e) illustrate how the smoothing technique reduces experimental noise in mode shapes obtained for one of the damaged scenarios considered in next sections.

As the wavelet transform needs a significant amount of points for the integration input signal so as to obtain meaningful coefficients and clear results, the reduction of required measuring points is a major challenge when applying space based wavelet transform to damage detection. If the number of experimental measurement points is not large enough, then an interpolation may be performed between the experimental values. In this paper a cubic spline interpolation technique is
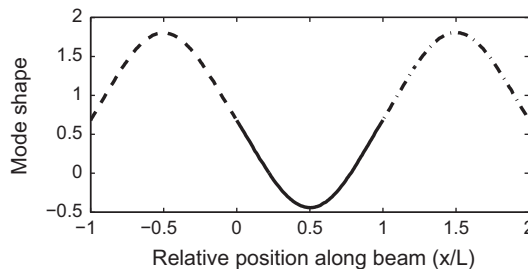

Fig. 2. Extension of the first mode shape of the free-free tested beam: original signal (solid line), left extension (dashed line) and right extension (dashed-dotted line).
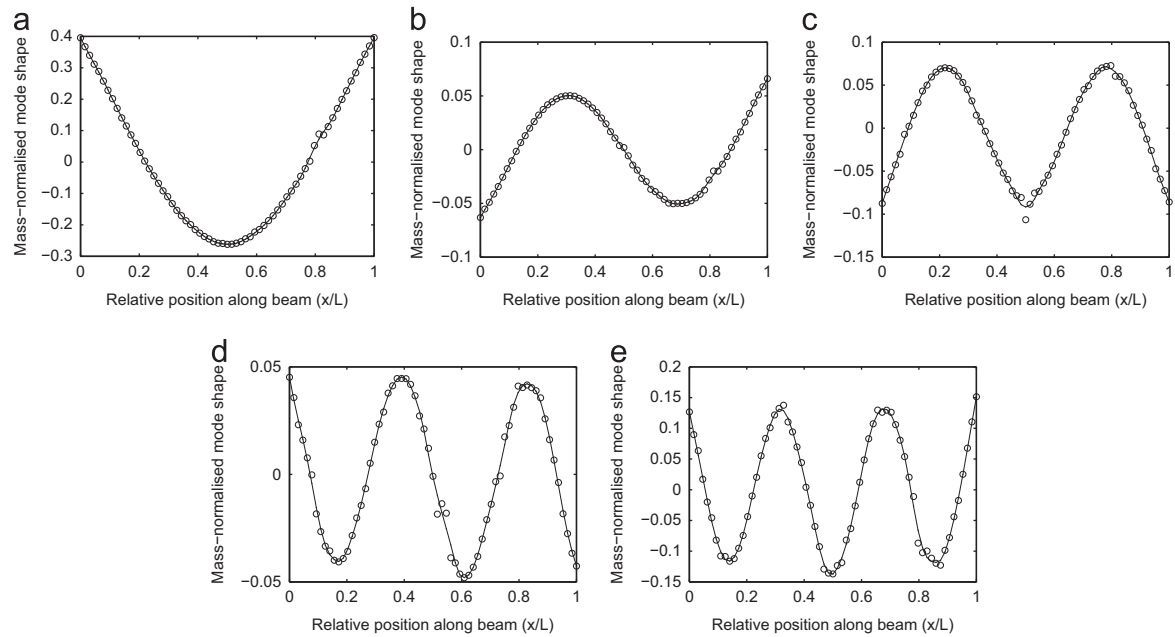
Fig. 3. Experimental mode shapes (dots) and smoothed mode shapes (solid line) for the free-free tested beam in scenario 3: (a) first mode shape, (b) second mode shape, (c) third mode shape, (d) fourth mode shape and (e) fifth mode shape.
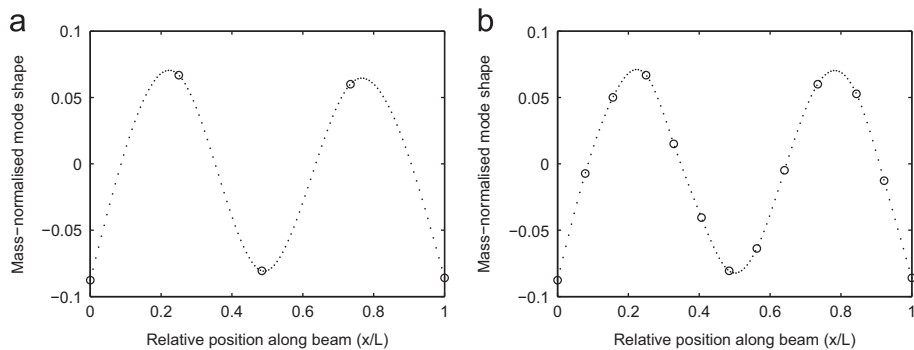

Fig. 4. Interpolated mode shapes (dotted line) and measuring points (circles) for mode 3 of scenario 3 from: (a) 5 points and (b) 13 points.

Table 1
Damage scenarios.

Scenario	Cutting location	Cut depth	Observation
0			Undamaged
1	0.5 L	30 mm	The full flange and part of the web are damaged
2	0.5 L	20 mm	
3	0.5 L	10 mm	10 mm cut at each side of the flanges and the web remains intact
4	0.4 L	30 mm	The full flange and part of the web are damaged
5	0.25 L	30 mm	
6	0.25 L	20 mm	
7	0.25 L	10 mm	10 mm cut at each side of the flanges and the web remains intact

applied [16,27]. Fig. 4 illustrates how the interpolation works if 5 or 13 measuring points were available and 128 interpolated points were obtained. The interpolation process smooths the resulting mode shape by itself, so the previously described smoothing technique based on a least squares regression is not necessary when interpolation is applied.

The interpolation technique is also needed when the measuring points are not uniformly distributed. The usual required uniform time sampling for Fourier or wavelet transform time domain applications is also required when geometric based transform is applied. Thus, the wavelet transform is always applied to a vector which components must be geometrical

equally spaced. Therefore, if the measuring points are not uniformly distributed along the structure, the interpolation can be used to obtain smooth mode shape vectors with equally distributed components.

The interpolation technique can also be used as a tool for disregarding measuring points where undesirable peaks are obtained for the mode shapes and they are clearly identified as noisy samples. When disregarding a measuring point, the resulting samples assemble may not be uniformly distributed so the interpolation technique may be used to circumvent that, as explained above.
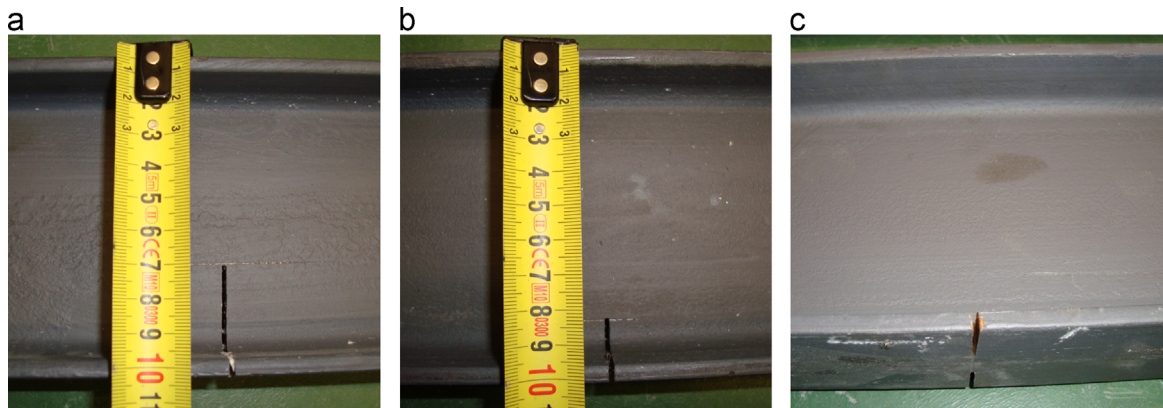
Fig. 5. Saw cut for considered scenarios: (a) 1, 4, 5, (b) 2, 6, and (c) 3, 7.
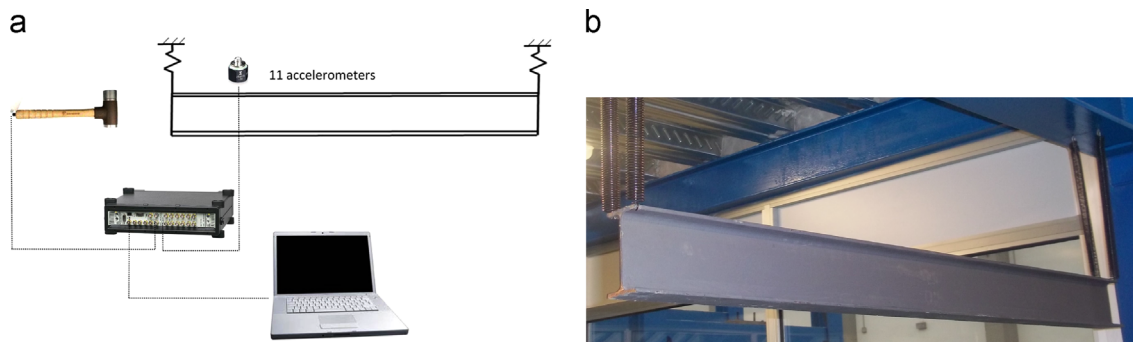
Fig. 6. (a) Experimental configuration and (b) test set-up in the laboratory.

Table 2
Experimental natural frequencies [Hz] for each damage scenario.

Mode \ scenario	0	1	2	3	4	5	6	7
1	415.65	300.96	362.28	407.57	310.17	364.75	397.27	415.0
2	1032.70	1027.35	1030.15	1033.32	949.64	822.99	932.71	1020.23
3	1786.75	1473.96	1634.17	1781.58	1650.20	1557.21	1663.19	1772.57
4	2581.50	2563.38	2576.63	2566.85	2445.3	2528.65	2556.50	2580.6
5	3366.63	3195.89	3253.80	3354.80	3080.5	3292.95	3354.27	3371.16

Table 3
MAC values for each damaged and the corresponding undamaged mode shape.

Mode \ scenario	1	2	3	4	5	6	7
1	0.99258	0.99795	0.99986	0.97986	0.96861	0.99413	0.99980
2	0.99874	0.99829	0.99825	0.96232	0.89482	0.96742	0.99785
3	0.93651	0.98433	0.99320	0.96880	0.85313	0.95711	0.99702
4	0.99214	0.99024	0.98549	0.95868	0.97374	0.98439	0.97250
5	0.94910	0.96810	0.98536	0.78420	0.95796	0.98317	0.99006

It is worth to mention that there should be always measuring points at both ends of the beam. If that is not the case, the portion of the beam to be analyzed should only be the portion defined by the distribution of the measuring points, so extrapolation is never done to infer the approached mode shape.
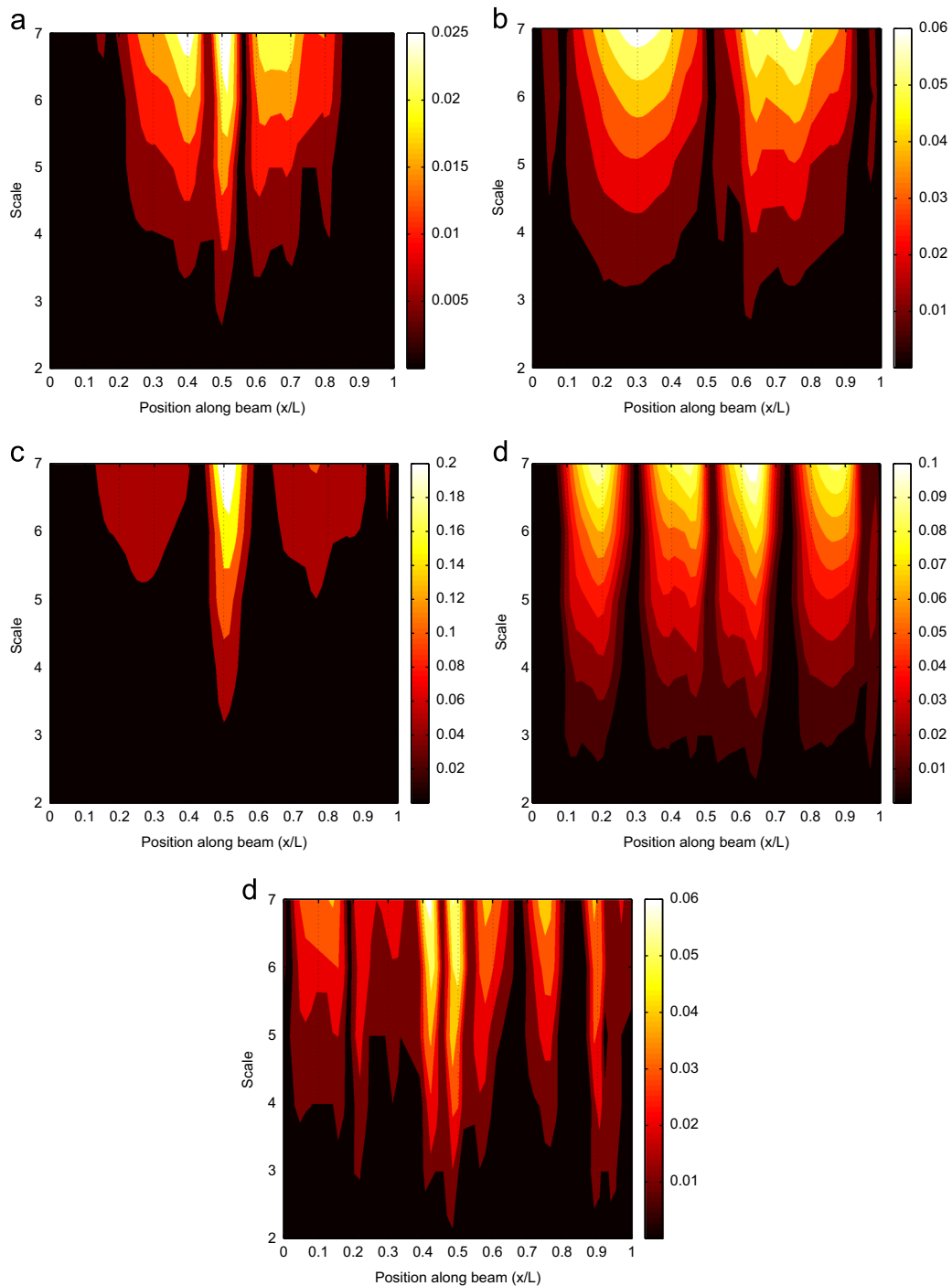

Fig. 7. Absolute values of CWT coefficients of mode shape difference for scenario 1 obtained from the response at 65 points: (a) mode shape 1, (b) mode shape 2, (c) mode shape 3, (d) mode shape 4 and (e) mode shape 5.

3.4. Wavelet transform of difference of modes

Once the extended and smoothed mode shapes have been obtained, the wavelet analysis is applied. Firstly, the extended difference mode shapes ($\Phi_{diff,ext}$) are obtained by computing the difference between the smoothed extended damaged
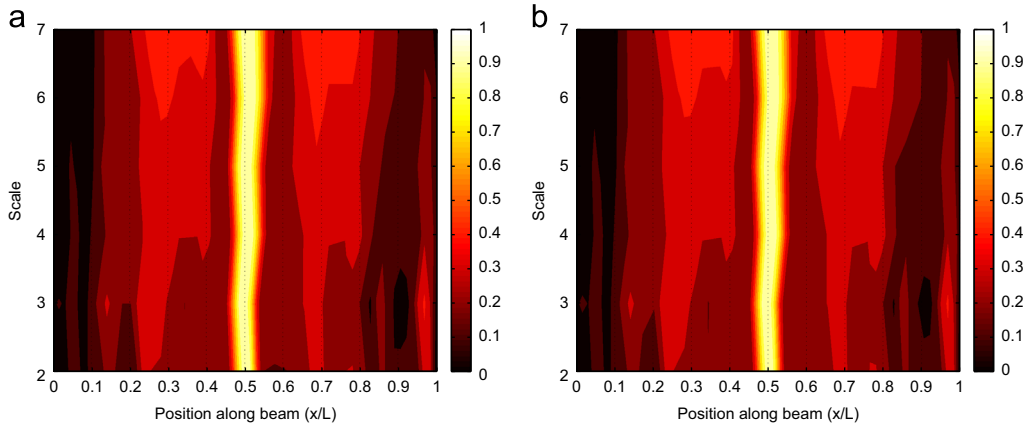

Fig. 8. Normalized weighted addition of CWT coefficients of mode shape difference for scenario 1 obtained from the smoothed and extended response at 65 points from: (a) three mode shapes and (b) five mode shapes.
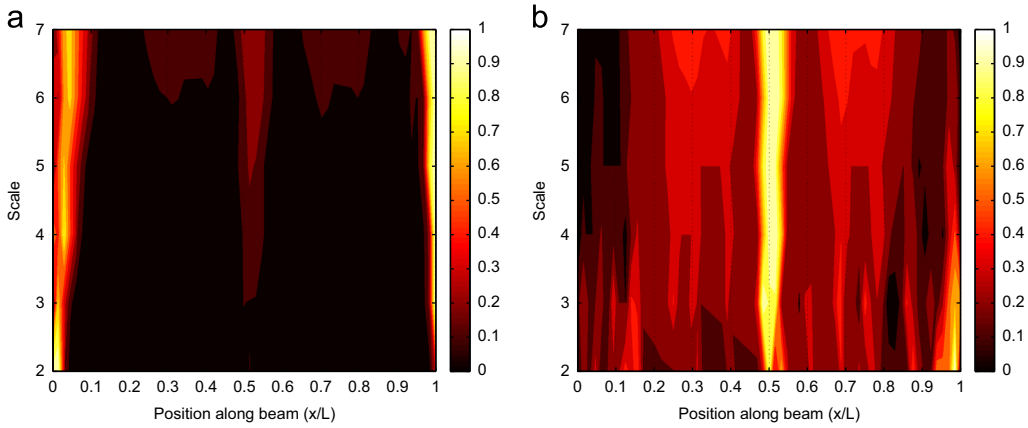

Fig. 9. Weighted addition of CWT coefficients of mode shape difference for scenario 1 obtained from the response at 65 points: (a) original signal and (b) extended signal.
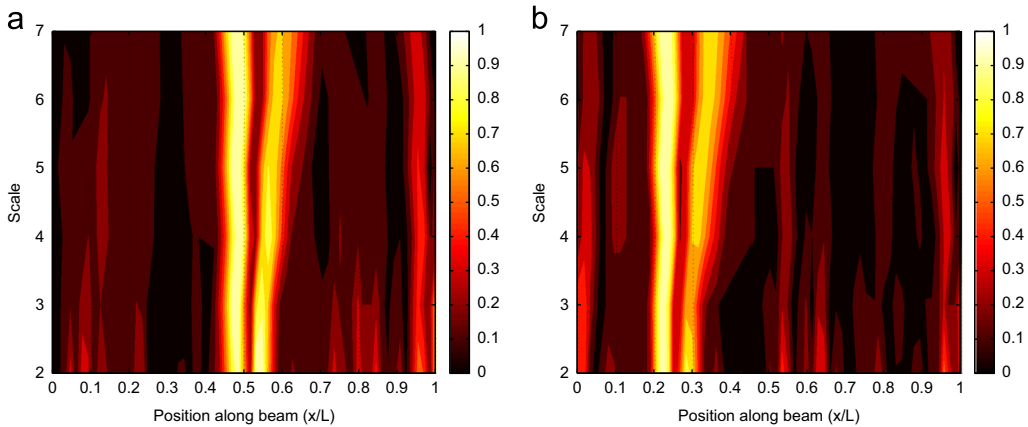

Fig. 10. Normalized weighted addition of CWT coefficients of mode shape difference obtained from the smoothed and extended response at 65 points using wavelet function Daubechies with 3 vanishing moments: (a) scenario 1 and (b) scenario 5.

$(\Phi_{s,ext,d})$ and undamaged $(\Phi_{s,ext,u})$ mode shapes:

$$\Phi_{diff,ext}(x) = (\Phi_{s,ext,d}(x) - \Phi_{s,ext,u}(x)) \tag{9}$$

Then, a CWT of each extended mode shape difference is done to give information about changes in mode shapes. The CWT for the ith mode shape can be written as

$$CWT^i_{\Phi_{diff,ext}}(u,s) = \frac{1}{\sqrt{s}} \int_{-\infty}^{+\infty} \Phi^i_{diff,ext}(x) \Psi^* \left(\frac{x-u}{s} \right) dx \tag{10}$$

It is proposed in this paper that the CWT is performed to a maximum scale (N_{scale}) that matches the maximum decomposition level that could be used if a multi-resolution DWT analysis [37] was applied according to the number of components of the extended mode shapes (N):

$$N_{scale} = \log_2(N) \tag{11}$$

From this point, only the CWT coefficients that corresponds to the original signal ($CWT_{\Phi_{diff}}$), and therefore to the real structure, will be considered.

3.5. Normalized weighted addition of wavelet results based on frequency changes

In order to simplify the analysis of the CWT for each mode shape and to draw an overall result for damage detection, the values of CWT coefficients of each mode shape are added up to obtain a global result for damage detection (Eq. (12)). The combination of the results for all mode shapes may also reduce the effect of noise that is present in a specific mode shape, whereas it will always accumulate the effect of damage for all mode shapes. For a more precise and clear detection of singularities, this paper proposes to combine and analyze the absolute values of the wavelet coefficients. In addition, the
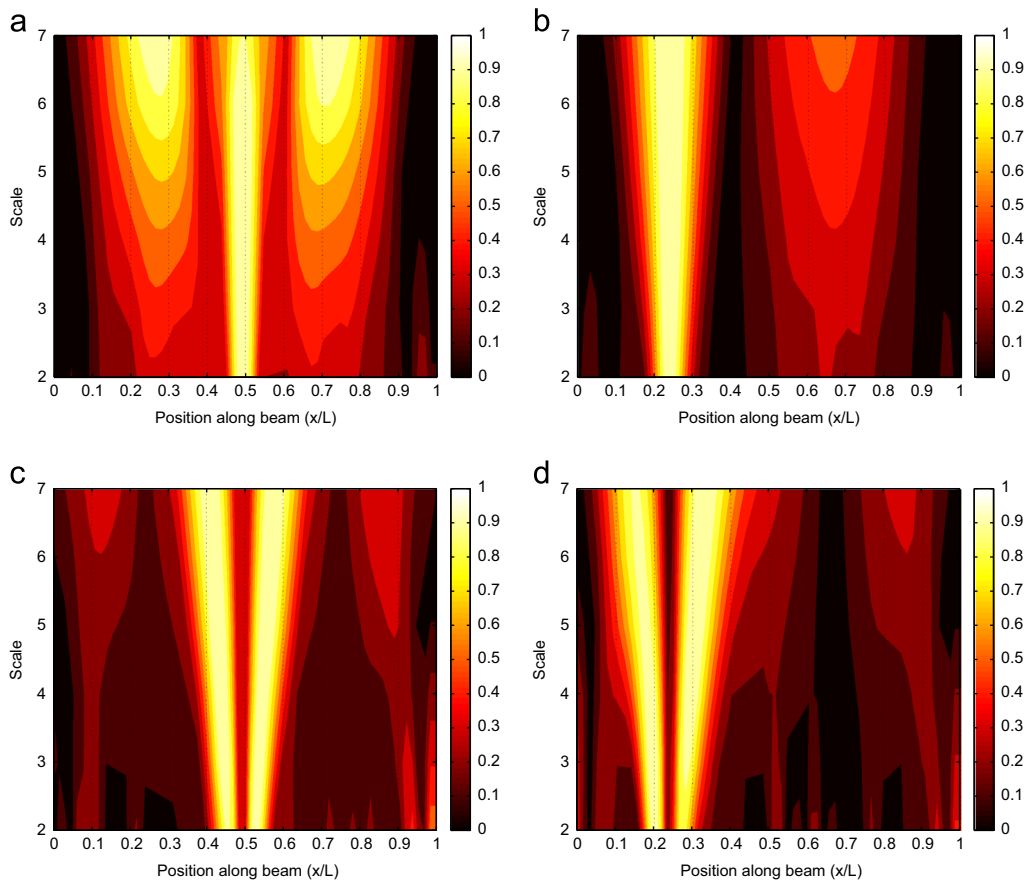

Fig. 11. Normalized weighted addition of CWT coefficients of mode shape difference obtained from the smoothed and extended response at 65 points using (a, b) wavelet function Gauss with 2 vanishing moments and (c, d) wavelet function Gauss with 3 vanishing moments: (a, c) scenario 1 and (b, d) scenario 5.

coefficients for each mode shape are weighted according to its corresponding change in natural frequencies:

$$CWT_{sum}(u,s) = \sum_{i=1}^{N} \left| CWT^i_{\Phi_{diff}}(u,s) \right| \cdot \left(1 - \frac{\omega^i_u}{\omega^i_d} \right)^2 \tag{12}$$

where ω^i_u and ω^i_d stand for the natural frequencies of mode shape i for the undamaged and the damaged state, respectively.

The weighting of the difference of the damaged and undamaged mode shapes with their natural frequencies relations is used to emphasize the most sensitive mode shapes to damage. It is assumed that those modes that exhibit a higher frequency change are more sensitive to damage and therefore changes in those mode shapes are more significant. On the other hand, the mode shapes that do not change their natural frequencies are almost disregarded. They are likely to introduce mainly noise in the final result when all the mode shapes are combined.

Finally, the resulting weighted addition of CWT coefficients is normalized to unity for each scale,

$$CWT_{sum-norm}(u,s) = \frac{CWT_{sum}(u,s)}{max[CWT_{sum}(u,s)]_s} \tag{13}$$

Normalized coefficients give a more clear final result since the information for all scales can be analyzed together.

3.6. Analysis of the results for damage detection and location

The normalized weighted addition of absolute values of CWT coefficients of mode shapes differences ($CWT_{sum-norm}(u,s)$) can be finally plotted so information for all scales is available along the beam in just one final figure. This figure, together with the representation of the results for each mode is analyzed in order to detect and locate damage.

The CWT of each mode shape difference can be used to detect damage. The instabilities in the CWT coefficients can indicate the location of damage. A ridge or increasing values with scale in the CWT coefficients can be interpreted as a structural damage effect [11,16,24]. In addition, the values of coefficients and singularities will be larger as the damage is
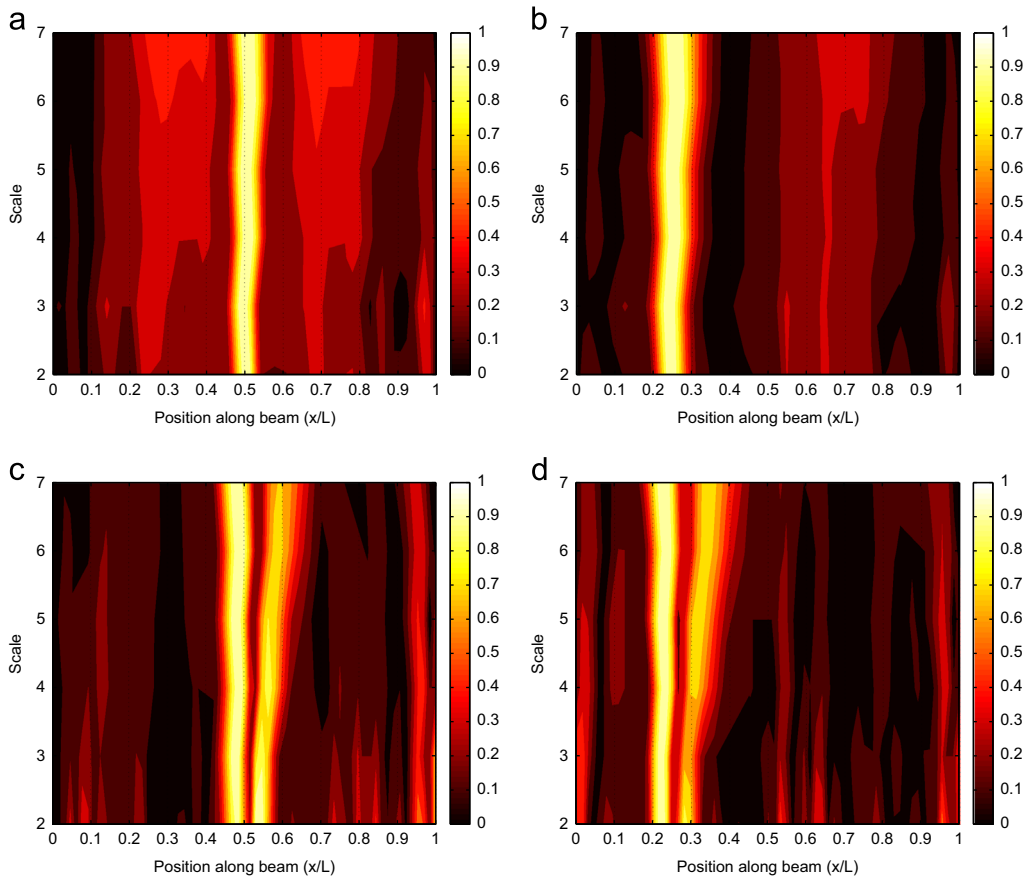

Fig. 12. Normalized weighted addition of CWT coefficients of mode shape difference obtained from the smoothed and extended response at 65 points using (a, b) wavelet function Symlet with 2 vanishing moments and (c, d) wavelet function Symlet with 3 vanishing moments: (a, c) scenario 1 and (b, d) scenario 5.

more severe. Therefore, comparing the results for different modes and for different damage scenarios can provide information about damage severity as well as information about sensitivity to damage of each mode.

Although the effect of damage produces larger values of coefficients for higher scales, the effect of damage is also present for lower scales. Therefore, when the coefficients from all modes are combined and normalized for each scale (Eq. (13)), the effect of damage can be noticed for all scales and is clearly detected when maximum values (unity) are obtained for every scale at a certain location. Without normalization, the information for lower scales is hidden.

It must be noted that, after normalizing, weighting and adding the absolute values of the CWT coefficients, the final coefficients are analyzed in order to detect singularities induced by damage, and not to interpret their exact mathematical or physical meaning. This analysis requires a deep mathematical analysis, which is out of the scope of the present paper. However, some remarks and ideas are discussed in the following paragraphs.

According to the definition of the CWT, the wavelet coefficients of the difference in mode shapes indicate how similar are the mode shapes differences to the wavelet function at each scale and for a certain location. They can also be interpreted in terms of wavelet energy [7], which is defined as the squared sum of all coefficients. The squared sum of the coefficients for a certain scale or for a certain location gives the wavelet energy for that scale or location, respectively.

However, the relation between wavelet coefficients and the derivatives of the original function is a more interesting feature for the application of wavelet analysis to mode shapes for damage detection. It can be mathematically demonstrated [37,44,45] that, when using certain wavelets (such as Gauss or Daubechies), the wavelet coefficients for lower scales are directly related to the derivatives of the original function of the same order as the number of vanishing moments of the wavelet function. Therefore, if a wavelet family with 2 vanishing moments is used, the CWT coefficients of mode shapes differences give information about the change in the second derivatives of mode shapes (modal curvatures). It is well known that change in modal curvatures is a sensitive damage detection parameter and it has been widely used in the literature since the pioneering proposal of Pandey [46]. Thus, the relation between the obtained wavelet coefficients using a Daubechies wavelet with 2 vanishing moments and the changes in modal curvatures justifies the sensitivity of the proposed methodology to damage.
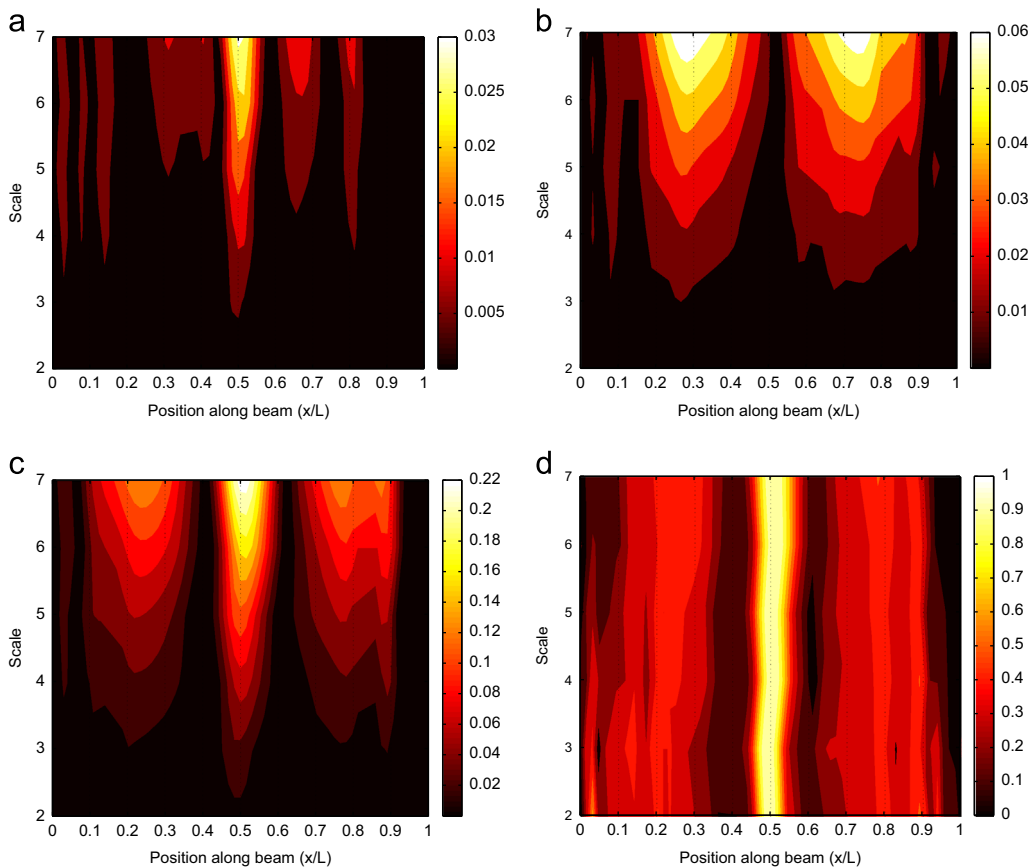

Fig. 13. CWT coefficients of mode shape difference for scenario 2 obtained from the response at 65 points: (a) mode shape 1, (b) mode shape 2, (c) mode shape 3 and (d)normalized weighted addition.

4. Experimental testing

Eight standard steel I-beams have been tested to apply the proposed methodology. The beams of length $L=1280$ mm, height $h=100$ mm, width $b=50$ mm, web thickness $h_w=4.5$ mm, flange thickness $h_f=6.8$ mm and mass per unit length $m=8.1$ kg/m have been damaged by a saw cut in the scenarios described in Table 1 and Fig. 5(a–c). The cuts are 1 mm width approximately.

The experimental program involved dynamic characterization of the specimens by modal analysis. An impact force was applied at one end of the beams by an instrumented impact hammer and the response was measured at 65 points distributed along the beam every $d=20$ mm. Piezoelectric accelerometers with nominal sensitivity of 100 mV/g and a low frequency limit of 2 Hz were used. The beams were hung in two soft springs at both ends with $k_s=145.8$ N/m stiffness, approaching a free-free boundary condition (Fig. 6).

Since a maximum of eleven accelerometers were available for the testing, seven set-ups were required to cover the 65 measurement points. For each set-up, several impacts were performed in order to eventually obtain average values and reduce the experimental noise effect. Impact response was acquired in 30 s per channel per set-up. The data were sampled to 16,384 Hz. After the experimental testing of the beams, the first five natural frequencies and mass normalized mode shapes were identified from impact vibration responses. Identified natural frequencies are in the range between 300 Hz and 3400 Hz. Fig. 3(a–e) show the mass normalized mode shapes for scenario 3. Table 2 presents the five natural frequencies that have been identified for each damage scenario. Table 3 shows the Modal Assurance Criteria values (MAC) [47] obtained between each damaged mode and the corresponding undamaged one, respectively.

Natural frequencies and MAC values decrease as the damage is more severe. Nevertheless, MAC values are always close to one, indicating that mode shapes are similar to those obtained for the undamaged state. Therefore, damage detection methodologies based on natural frequency change or MAC values could only detect damage in the most severe scenarios. In the next section, the proposed methodology is used to detect as well as to locate damage.
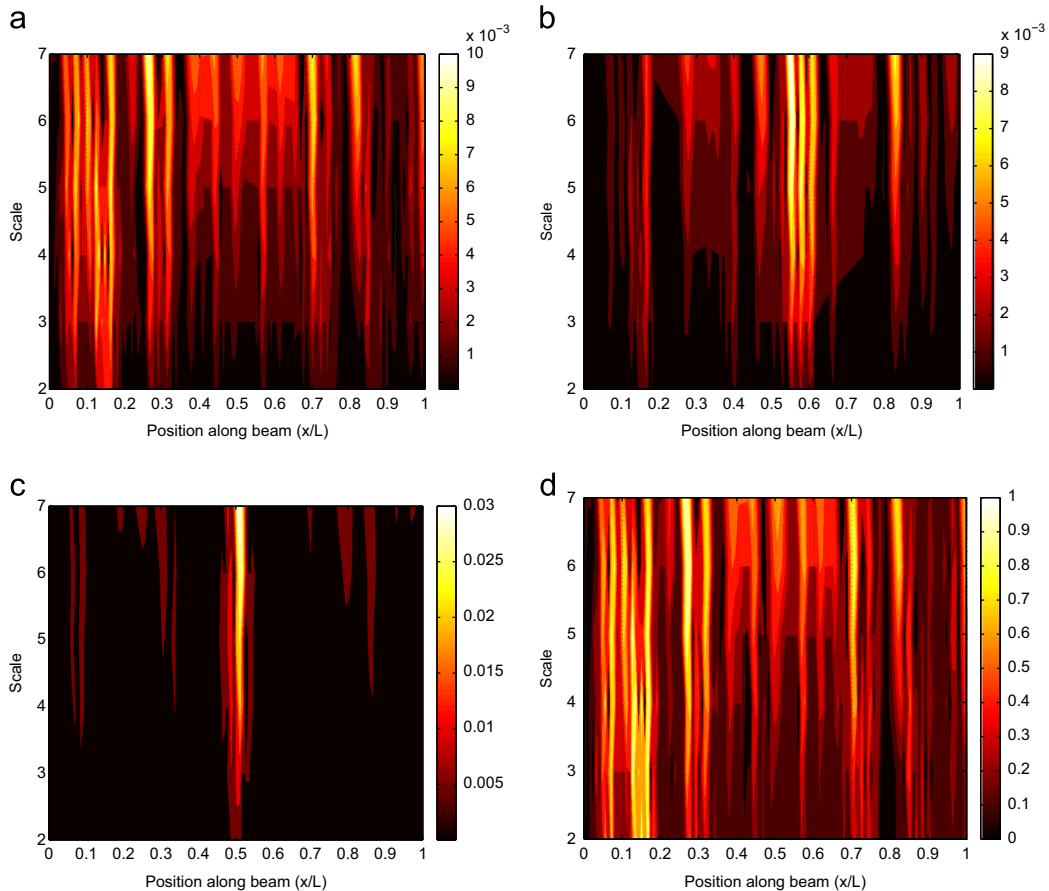

Fig. 14. CWT coefficients of mode shape difference for scenario 3 obtained from the response at 65 points: (a) mode shape 1, (b) mode shape 2, (c) mode shape 3 and (d) normalized weighted addition.

Mode shapes 2 and 4 have a node at the middle length of the beam so they are not sensitive to damage at that location. Therefore, only changes of the odd mode shapes will determine damage detection at 0.5 L. It can be observed in Tables 2 and 3 that natural frequencies and MAC values remain almost constant for mode shapes 2 and 4 in scenarios 1, 2 and 3.

5. Results

This section presents the results obtained when the proposed combined modal wavelet methodology is applied to the experimentally tested beams. Moreover, several aspects that may influence the final results are discussed, such as the effect of the numerical manipulations of the original experimental mode shapes (extension and curve fitting), the choice of the wavelet family, the number of modes considered and the number of measuring points.

Fig. 7 shows the absolute values of CWT coefficients of the extended difference of modes 1–5 (Eq. (10)) for scenario 1. The absolute values of the coefficients are presented for different scales along the beam in each figure. It can be noticed from Fig. 7(b,d) that modes 2 and 4 are not sensitive to damage at 0.5 L, since there is a node at that position. Their CWT coefficients are larger at those parts of the beam which show higher modal amplitudes for the second and fourth bending mode, respectively. Therefore, those high values are induced by the intrinsic mode shape nature and not by damage. On the other hand, modes 1, 3 and 5 (Fig. 7(a,c,e)) are sensitive to damage at 0.5 L. They show a narrow band of increasing values with scale at damage location.

The normalized weighted addition of the coefficients of Fig. 7 (Eq. (13)) is presented in Fig. 8(a,b) considering 3 and 5 modes respectively. Fig. 8 shows that the normalized weighted addition of the wavelet coefficients gives a much more clear result for damage detection than the CWT coefficients of each mode (Fig. 7). The weighted addition make emphasis on those modes that are more sensitive to damage (modes 1, 3 and 5 according to the change in natural frequencies). The normalization of the coefficients provides complete information about the effect of damage for every scale. Fig. 8 shows that the effect of damage consists of high values (unity) around the damage position for every scale. Both Fig. 8(a,b) are almost identical, so no improvement in the final result is achieved by including the fourth and fifth modes. Analogous results are obtained for all scenarios. Therefore, the results for the rest of the paper are analyzed for only 3 modes, since from a practical point of view, requiring a small number of mode shapes for damage detection is advantageous.
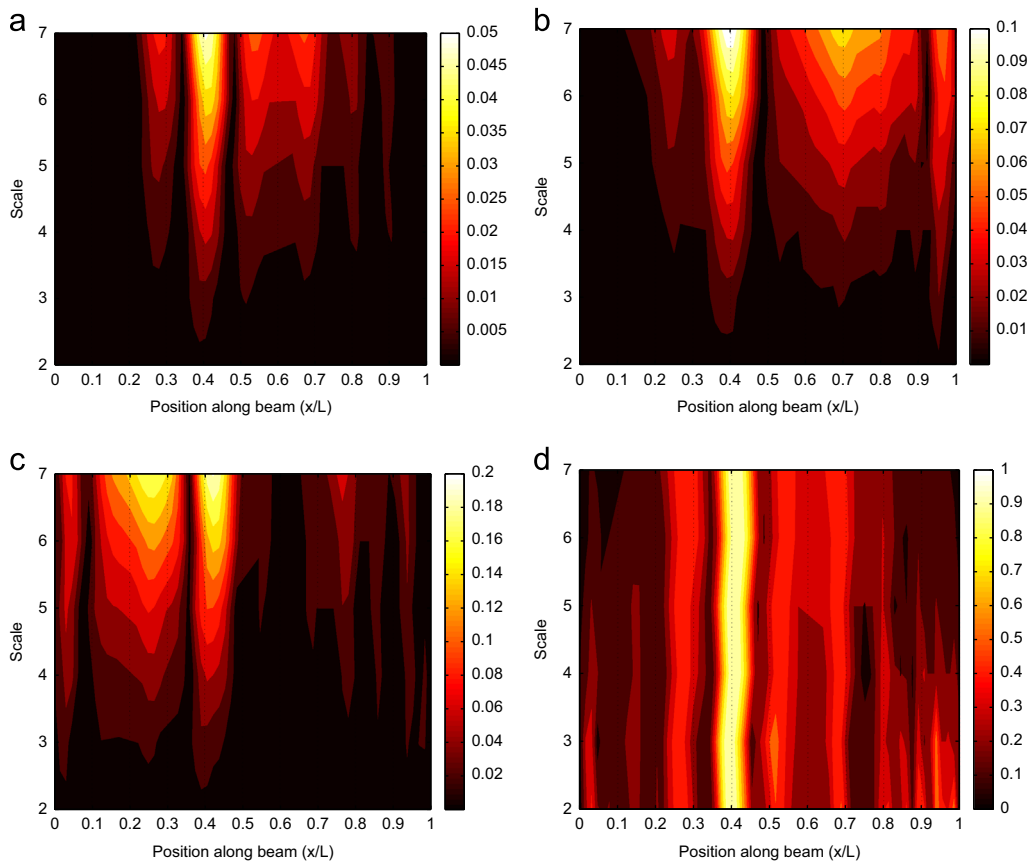

Fig. 15. CWT coefficients of mode shape difference for scenario 4 obtained from the response at 65 points: (a) mode shape 1, (b) mode shape 2, (c) mode shape 3 and (d) normalized weighted addition.

In order to illustrate the effect of the extension and the curve fitting of mode shapes to reduce the edge effect and experimental noise, Fig. 9 shows how both techniques affect the final results. Fig. 9(a) shows the normalized weighted addition of the CWT coefficients of the experimental mode shapes, without neither applying extension nor curve fitting. It can be observed that because of the edge effect the highest values are located at the beginning and at the end of the beam and they mask the effect of damage. After applying the extension (Fig. 9(b)), the edge effect disappears and the effect of damage is clear at 0.5 L. When the curve fitting approach is also applied, the final result depicted in Fig. 8(a) is obtained, which is very similar to that of Fig. 9(b). However, the curve fitting smooths the mode shapes without eliminating the effect of damage so there is less noise effect in Fig. 8(a) and the effect of damage is even more clear.

As it was mentioned above, the choice of the wavelet function and its number of vanishing moments affects the sensitivity of the wavelet transform to damage. Fig. 10 shows the normalized weighted addition of CWT coefficients of difference in mode shapes using a Daubechies wavelet function with 3 vanishing moments for scenarios 1 and 5. By comparing Fig. 10(a,b) with Figs. 8(a) and 16(d) it can be observed that the effect of damage is identified using both Daubechies wavelets with 2 and 3 vanishing moments but it is more clearly detected and the resolution of damage location is much better when using 2 vanishing moments. According to Section 3.6, the Daubechies wavelet with 2 vanishing moments is sensitive to changes in modal curvatures whereas the wavelet with 3 vanishing moments is sensitive to the third derivatives of mode shapes differences. As a result, due to its more oscillatory nature, the wavelet Daubechies wavelet with 3 vanishing moments gives maximum values at two different areas at each side of the location of damage, so the resolution for the location of damage is worst than the resolution when using 2 vanishing moments. Similar conclusions can be drawn for the Gauss and Symlet wavelets when using 2 and 3 vanishing moments (Figs. 11 and 12). Comparison of the results obtained with Daubechies, Gauss and Symlet wavelets shows that Daubechies wavelet is more sensitive to damage and provides better results, so Daubechies wavelet with 2 vanishing moments is chosen as the best candidate for being sensitive to the existence of a crack in the tested beams.

Figs. 13–18 show the CWT coefficients for the differences of the first three mode shapes and the cumulative normalized weighted addition for scenarios 2–7, respectively, using the experimental mode shape measured at 65 points. As previously mentioned, large values (unity) of the CWT coefficients at a certain location and for every scale can be interpreted as damage effect.
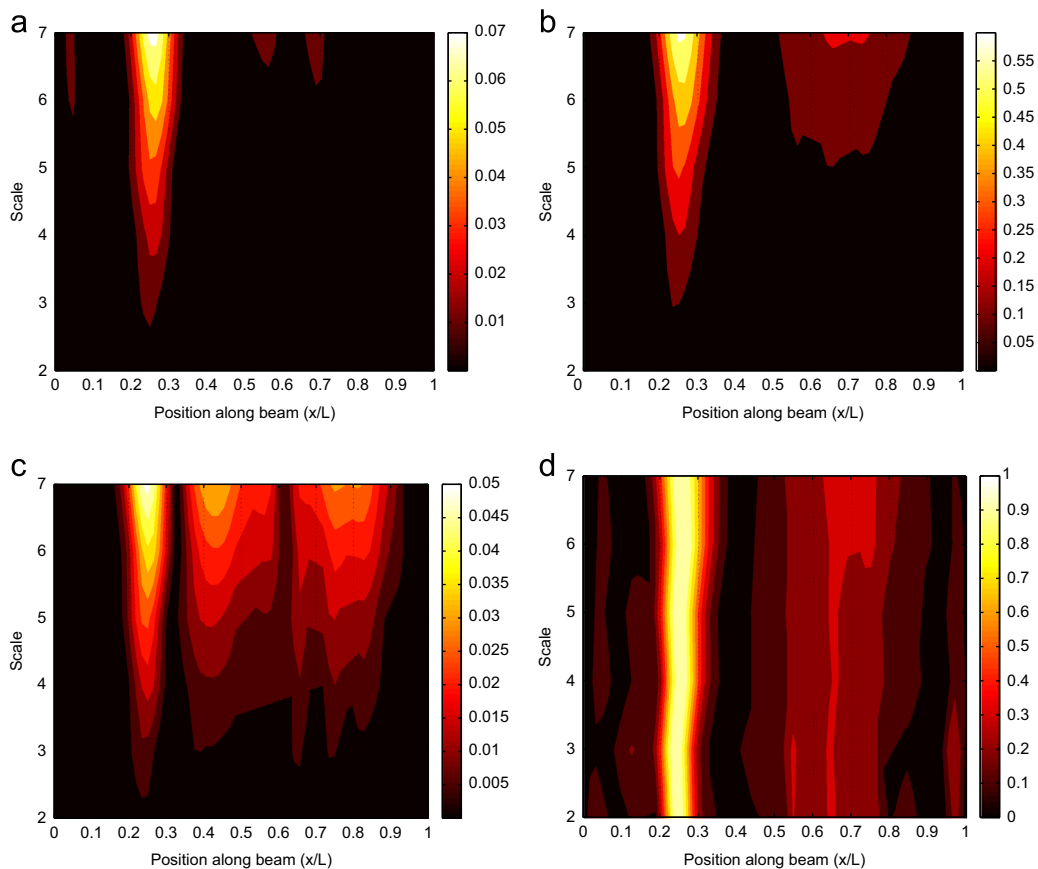

Fig. 16. CWT coefficients of mode shape difference for scenario 5 obtained from the response at 65 points: (a) mode shape 1, (b) mode shape 2, (c) mode shape 3 and (d) normalized weighted addition.

Fig. 13 shows that damage scenario 2 can be successfully identified from the CWT values of the first and third mode and even more clearly identified from the normalized weighted addition of coefficients. The less severe damage at 0.5 L (scenario 3) cannot be detected from Fig. 14(a)–(d). Irregular distribution of high values in the figures are produced mainly by noise. It is worth to mention that mode 3 seems to be detecting damage but the CWT high values at 0.5 L are actually induced by noise. It can be observed in Fig. 3(c) that an inaccurate modal amplitude sample is obtained at that location from the experimental tests. However, the weighted addition of results for all mode shapes eliminates the influence of that noisy sample, although the effect of damage is definitely masked by the effect of noise, which contaminates the result all along the beam.

When damage is located at 0.4 L (Fig. 15) the effect of damage is clear at that position for mode shapes 1 and 2, and even more clear from the normalized weighted addition of CWT coefficients.

The analysis of the results for damage at 0.25 L (Figs. 16–18, corresponding to scenarios 5, 6 and 7, respectively) shows that all the three mode shapes are sensitive to damage at that location. Mode shape 2 shows the highest decrease in natural frequency and the highest CWT values are obtained for that mode, so it is the most sensitive mode shape to damage. Damage is clearly located and indicated for all mode shapes and their corresponding addition for scenarios 5 and 6 (Figs. 16 and 17, respectively). The results for scenario 7 (Fig. 18) can not reveal the presence of damage. High CWT values are spread along the beam at different scales, so the effect of noise is affecting the results more than the damage do, as it occurs for scenario 3 (Fig. 14).

In order to illustrate the spatial resolution of the proposed methodology for damage location, Fig. 19 shows the obtained CWT coefficients for different scales for scenarios 1 and 5. It shows that the location of the maximum value of the normalized weighted addition of CWT coefficients varies with the scale. In addition, the width of the area where the coefficients are higher increases with the scale and, therefore, the resolution for damage location is lower for higher scales. This phenomenon explains why the stripes of maxima values of the figures presenting the normalized weighted addition of CWT coefficients are not strictly perpendicular to the horizontal axis. It also explains why these stripes are wider for higher scales and show some conical appearance. Nevertheless, it can be seen that the methodology provides good resolution for damage. According to the distribution of the maximum values, the resolution of the proposed methodology can be estimated as 40 mm (twice the separation between sensors) for the damage location for the tested beams.
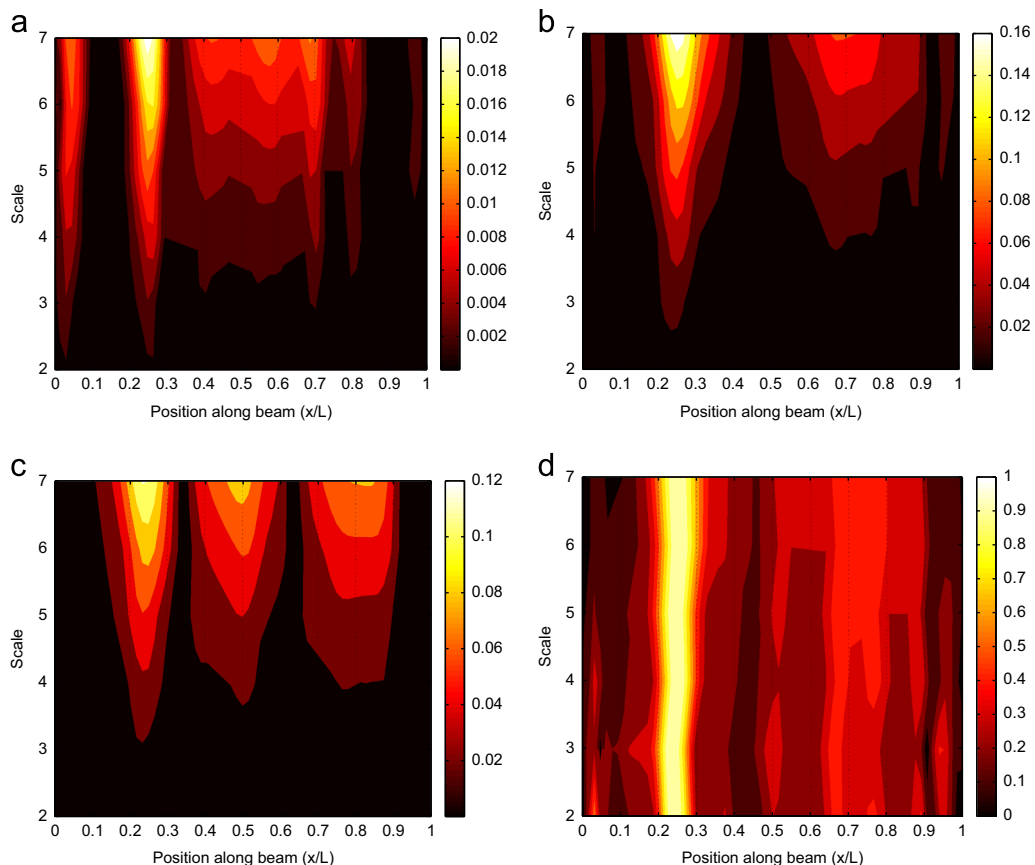

Fig. 17. CWT coefficients of mode shape difference for scenario 6 obtained from the response at 65 points: (a) mode shape 1, (b) mode shape 2, (c) mode shape 3 and (d) normalized weighted addition.

As mentioned in Section 3.6, it can be observed from Figs. 7, 13–17 and 18(a–c) that CWT values of mode shape difference increase with the severity of damage (size of the crack), since the difference of mode shapes also increase with damage severity. However, information about damage severity from those figures can be only obtained in a qualitative and relative sense. A quantitative interpretation could only be feasible from a previous parametric analysis from numerical or analytical simulations along with experimental validations [18,28,48,49]. However, this kind of analysis is only valid for a specific application and can not be extrapolated to more general situations.
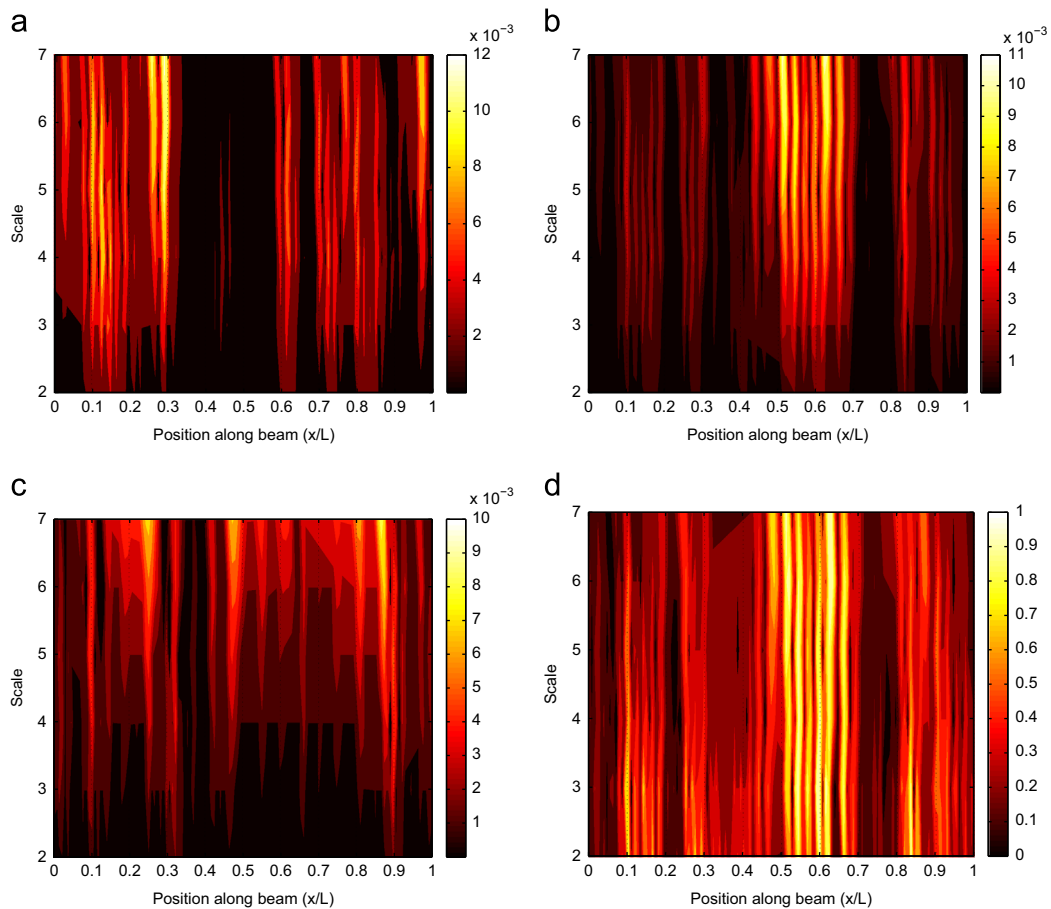

Fig. 18. CWT coefficients of mode shape difference for scenario 7 obtained from the response at 65 points: (a) mode shape 1, (b) mode shape 2, (c) mode shape 3 and (d) normalized weighted addition.
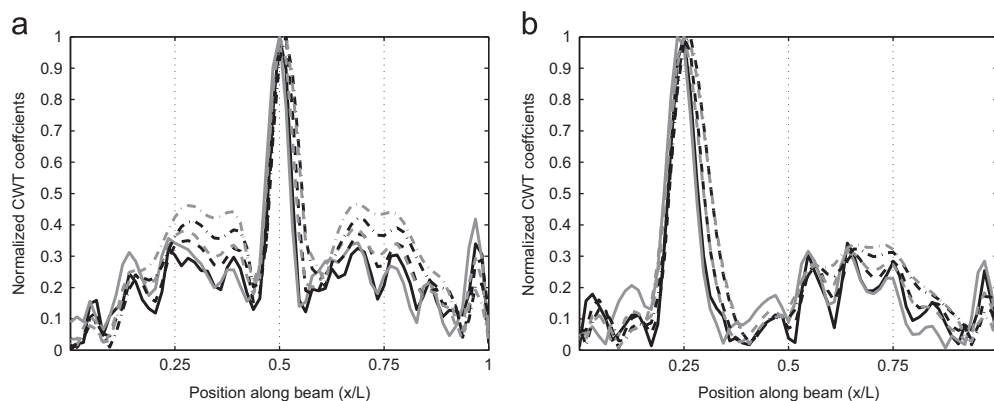

Fig. 19. Normalized weighted addition of CWT coefficients of mode shape differences for scenarios (a) 1 and (b) 5 using wavelet function Daubechies with 2 vanishing moments, obtained from scale 2 (black solid line), scale 3 (gray solid line), scale 4 (black dashed line), scale 5 (gray dashed line), scale 6 (black dash dotted line) and scale 7 (gray dash dotted line).

In order to analyze the number of measuring points required for damage detection and the effect of the proposed interpolation technique, only some of the original 65 measuring points were considered for all scenarios. The cumulative CWT results obtained from the response at 5 and 13 measuring points for damage located at 0.5 L, 0.4 L and 0.25 L are shown in Figs. 20–22, respectively. The interpolation technique is used to obtain approached mode shapes vectors of 128 components.

Fig. 20(b,d) show that damage could be located with 13 points as precisely as with the original 65 points when damage is located at 0.5 L. If the number of measuring points is reduced to 5 (Fig. 20(a,c)), then damage is not clearly located and its effect is masked by the high CWT values at high modal amplitudes areas of mode shapes. For the less severe damage scenario at 0.5 L (Fig. 20(e,f)), neither 5 nor 13 measuring points can detect damage. However, results are better than those obtained with 65 points, probably due to the fact that noisy samples are eliminated and noise effect is more effectively
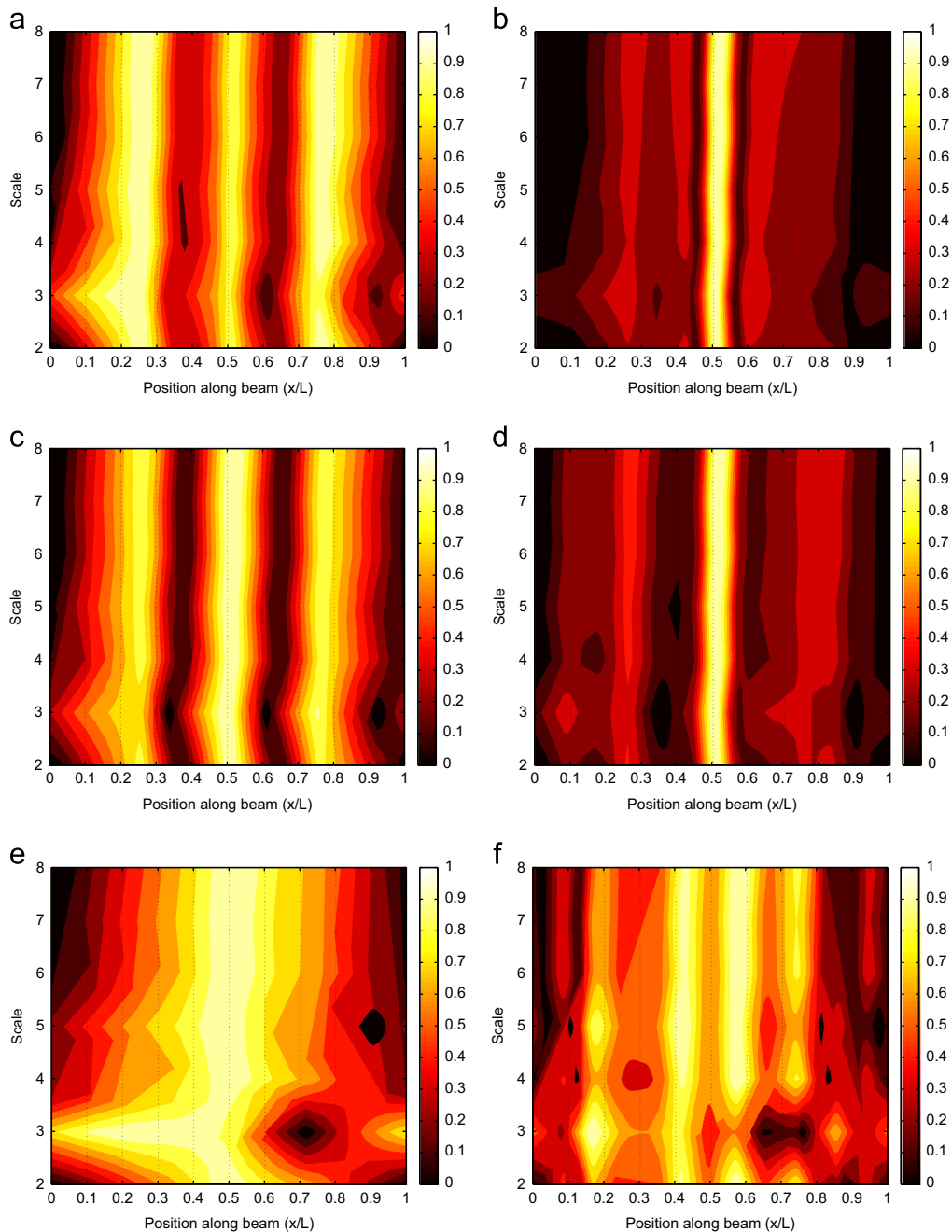

Fig. 20. Weighted addition of CWT coefficients of modes shapes differences obtained for (a, b) scenario 1, (c, d) scenario 2 and (e, f) scenario 3: (a, c, e) 5 measuring point and (b, d, f) 13 measuring points.
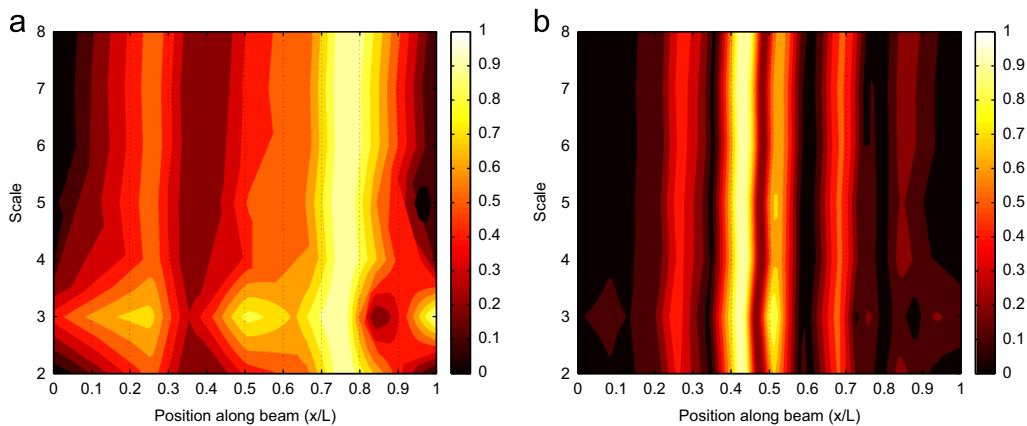
Fig. 21. Weighted addition of CWT coefficients of modes shapes differences obtained for scenario 4: (a) 5 measuring points, (b) 13 measuring points.

reduced. Thus, identifying and disregarding experimental mode shape amplitude samples that are clearly inaccurate may enhance the damage detection sensitivity and may be important to detect little damage. Nevertheless, the proposed methodology is not robust at this damage level yet.

When damage is located at 0.4 L (Fig. 22), the crack can also be located with 13 measuring points but not with 5. However, it can be noticed that the location of damage with 13 measuring points is not so accurate as with 65 points.

When damage is located at 0.25 L, similar conclusions to the 0.5 L damage location can be drawn. However, results are better since damage can be clearly detected for scenarios 5 and 6 even with only 5 measuring points (Fig. 22(a,c)), although the location of damage is more accurate when using more measuring points. For the less severe damage scenario (Fig. 22(e, f)), results are also better to those obtained with 65 measuring points, but also 'false damages' could be identified around 0.5 L and 0.75 L.

The number of measuring points as well as their location affects the damage detection sensitivity. In order to illustrate this, Fig. 23(a,b) show the weighted addition of CWT coefficients of mode shape differences along the beam for scale 7 and different numbers of measuring points (from 13–17), for scenarios 1 and 5 respectively. Scale 7 is selected since the largest values are obtained for the highest scales. Nevertheless, results for any other scale are similar. The singular behavior of the coefficients at damage location is clearly observed at Fig. 23(a,b). The proposed damage detection methodology is more sensitive to damage as the peak in CWT coefficients at damage location is more significant. It can be noticed from Fig. 23 that the peak is more significant when damage is at 0.25 L, so damage is more clearly detected at that position, as it has been shown from the results previously discussed.

In theory, in absence of noisy samples that could distort the results, the CWT values decrease with the number of measuring points. This is due to the fact that as the number of measuring points is reduced, less information is available and the effect of damage on the interpolated mode shapes is also reduced. However, this theoretical trend is perturbed by the fact that sensitivity increases when a sensor is located at damage location. When damage is located at 0.5 L, a sensor is located at that position when the number of sensors is odd, since the sensors are uniformly distributed along the beam. As a result, Fig. 23(a) shows that the CWT values with 13 measuring points is less than when using 15 but larger than when using 14. When damage is located at 0.25 L, a sensor is located at that position when the number of sensors is 5, 9, 13, 17, 21..., etc. Thus, maximum values of CWT coefficients decreases from using 13 to 15 measuring points, whereas they increase from 15 to 17 (Fig. 23(b)).

Previously presented results are successful for 13 sensors and even with 5 measuring points for certain scenarios, but it must be noted that a sensor is located at damage position when the crack is at 0.25 L and 0.5 L. However, results are also successful when damage is at 0.4 L when using 65 as well as 13 measuring points, despite no sensor is located at damage location. It can be concluded that results with less than 13 sensors may be successful or not depending on the damage scenario. Damage will be detected with 13 or more measuring points.

6. Conclusions

A new combined modal-wavelet analysis for crack location in beams has been successfully applied. The methodology is simple and easy to use. Behavior of coefficients of the wavelet transform at different scales are used to identify changes in mode shapes induced by damage. The wavelet space based transform is applied to the difference between obtained mode shapes of a potentially damaged beam and those corresponding to a reference state. The results for each mode are added up to give a final single result from which damage can be detected and located at a glance. However, wavelet results from each mode shape should also be considered for a more precise analysis.
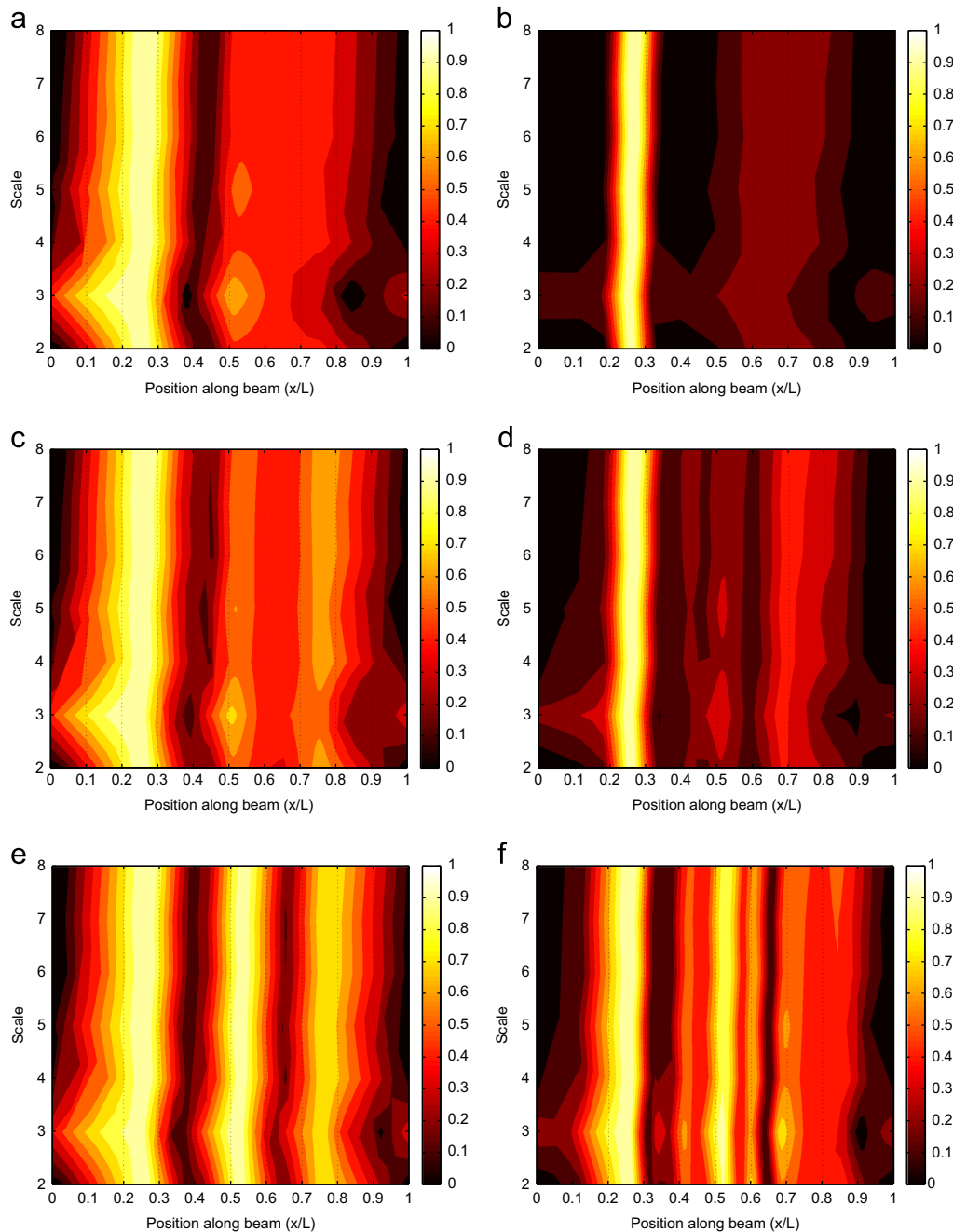
Fig. 22. Weighted addition of CWT coefficients of modes shapes differences obtained for (a, b) scenario 5, (c, d) scenario 6 and (e, f) scenario 7: (a, c, e) 5 measuring points and (b, d, f) 13 measuring points.

When adding up mode results, each one is weighted according to the natural frequency change from the reference value so modes that are likely to be sensitive to damage are emphasized. Finally, the coefficients are normalized for each scale so information for all the scales is analyzed in the same way and the effect of damage is more clear.

The proposed methodology includes a curve fitting approach to reduce the effect of experimental noise in mode shapes, so noise effect is not considered as actual damage and 'false damages' are avoided. The smoothing technique is based on a quadratic weighted regression for a moving span of ten points. Moreover, when a small number of sensors are used, new mode shape points are obtained from a cubic spline interpolation so enough points can be used to define the input signal for the wavelet transform. This interpolation also serves as a smoothing process when it is applied.

The new methodology has proven to be sensitive to little damage. According to the different locations and severity of damage in the beams experimentally tested, an estimated threshold value for damage detection could be defined by a
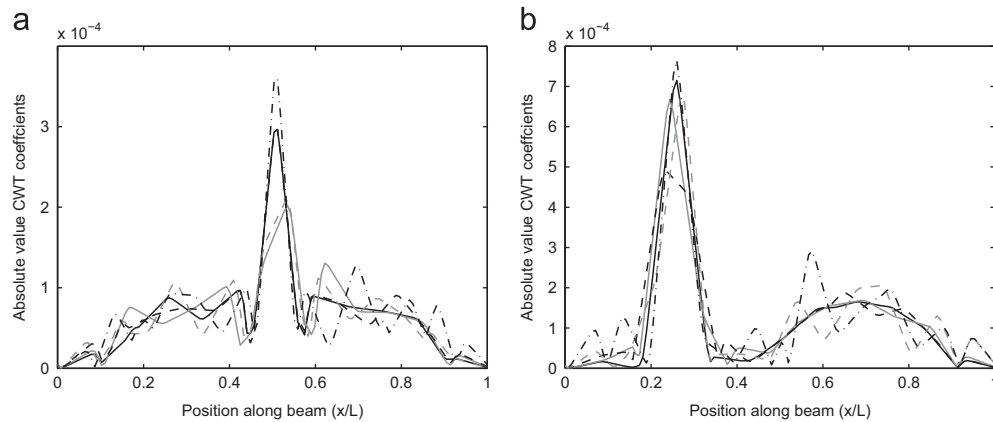
Fig. 23. Weighted addition of CWT coefficients for scale number 7 of mode shape differences for scenarios (a) 1 and (b) 5, obtained from 13 measuring points (black solid line), 14 points (gray solid line), 15 points (black dashed line), 16 points (gray dashed line) and 17 points (black dash dotted line).

change in natural frequencies of 8%. More severe damages will certainly be detected. It has also been shown that damage can be located using a rather small number of sensors and using a small number of mode shapes. Damage above the previously defined threshold value can be detected with only 13 sensors distributed along the beam and using only 3 bending modes.

Acknowledgements

References

[1] S. Doebling, C. Farrar, M. Prime, D. Shevitz, Damage identification and health monitoring of structural and mechanical systems from changes in their vibration characteristics: a literature review, Los Alamos National Lab., NM, United States.
[2] W. Fan, P. Qiao, Vibration-based damage identification methods: a review and comparative study, Struct. Health Monit. 10 (1) (2011) 83–111.
[3] A. Haar, Zur theorie der orthogonalen funktionensysteme, Math. Ann. 69 (3) (1910) 331–371.
[4] C. Surace, R. Ruotolo, Crack detection of a beam using the wavelet transform, in: Proceedings of the 12th International Modal Analysis Conference, 1994, pp. 1141–1147.
[5] M.M.R. Taha, A. Noureldin, J.L. Lucero, T.J. Baca, Wavelet transform for structural health monitoring: a compendium of uses and features, Struct. Health Monit. 5 (3) (2006) 267–295.
[6] H. Kim, H. Melhem, Damage detection of structures by wavelet analysis, Eng. Struct. 26 (3) (2004) 347–362.
[7] W.X. Ren, Z. Sun, Structural damage identification by using wavelet entropy, Eng. Struct. 30 (10) (2008) 2840–2849.
[8] H. Sohn, G. Park, J.R. Wait, N.P. Limback, C.R. Farrar, Wavelet-based active sensing for delamination detection in composite structures, 2004, http://dx.doi.org/10.1088/0964-1726/13/1/017.
[9] X. Deng, Q. Wang, V. Giurgiutiu, Structural health monitoring using active sensors and wavelet transforms, in: SPIE's 6 th Annual International Symposium on Smart Structures and Materials, Paper # 3667-35, 1999, pp. 1–5.
[10] G. Yan, Z. Duan, J. Ou, A.D. Stefano, Structural damage detection using residual forces based on wavelet transform, Mech. Syst. Signal Process 24 (1) (2010) 224–239.
[11] M. Rucka, K. Wilde, Application of continuous wavelet transform in vibration based damage detection method for beams and plates, J. Sound Vib. 297 (3–5) (2006) 536–550.
[12] K.M. Liew, Q. Wang, Application of wavelet theory for crack identification in structures, J. Eng. Mech.-ASCE 124 (2) (1998) 152–157.
[13] Q. Wang, X. Deng, Damage detection with spatial wavelets, Int. J. Solids Struct. 36 (23) (1999) 3443–3468.
[14] S. Quek, Q. Wang, L. Zhang, K.K. Ang, Sensitivity analysis of crack detection in beams by wavelet technique, Int. J. Mech. Sci. 43 (12) (2001) 2899–2910.
[15] A.V. Ovanesova, L.E. Suárez, Applications of wavelet transforms to damage detection in frame structures, Eng. Struct. 26 (1) (2004) 39–49.
[16] M. Rucka, K. Wilde, Crack identification using wavelets on experimental static deflection profiles, Eng. Struct. 28 (2) (2006) 279–288.
[17] N. Wu, Q. Wang, Experimental studies on damage detection of beam structures with wavelet transform, Int. J. Eng. Sci. 49 (3) (2011) 253–261.
[18] P. Umesha, R. Ravichandran, K. Sivasubramanian, Crack detection and quantification in beams using wavelets, Comput.-Aided Civil Infrastruct. Eng. 24 (8) (2009) 593–607.
[19] P.D. Spanos, G. Failla, A. Santini, M. Pappatico, Damage detection in Euler–Bernoulli beams via spatial wavelet analysis, Struct. Control Health Monit. 13 (1) (2006) 472–487.
[20] U.P. Poudel, G. Fu, J. Ye, Structural damage detection using digital video imaging technique and wavelet transformation, J. Sound Vib. 286 (4–5) (2005) 869–895.
[21] S. Zhong, S.O. Oyadiji, Crack detection in simply supported beams without baseline modal parameters by stationary wavelet transform, Mech. Syst. Signal Process. 21 (4) (2007) 1853–1884.
[22] C. Hu, M. Afzal, A wavelet analysis-based approach for damage localization in wood beams, J. Wood Sci. 52 (5) (2006) 456–460.
[23] S. Zhong, S.O. Oyadiji, Detection of cracks in simply-supported beams by continuous wavelet transform of reconstructed modal data, Comput. Struct. 89 (1–2) (2011) 127–148.
[24] E. Douka, S. Loutridis, A. Trochidis, Crack identification in beams using wavelet analysis, Int. J. Solids Struct. 40 (13–14) (2003) 3557–3569.
[25] C. Chang, L. Chen, Detection of the location and size of cracks in the multiple cracked beam by spatial wavelet based approach, Mech. Syst. Signal Process. 19 (1) (2005) 139–155.

[26] H. Gokdag, O. Kopmaz, A new damage detection approach for beam-type structures based on the combination of continuous and discrete wavelet transforms, J. Sound Vib. 324 (3–5) (2009) 1158–1180.

[27] M. Radzieński, M. Krawczuk, M. Palacz, Improvement of damage detection methods based on experimental modal parameters, Mech. Syst. Signal Process. 25 (6) (2011) 2169–2190.

[28] J. Xiang, M. Liang, Wavelet-based detection of beam cracks using modal shape and frequency measurements, Comp.-Aided Civil Infrastruct. Eng. 27 (6) (2012) 439–454.

[29] J. Xiang, T. Matsumoto, Y. Wang, Z. Jiang, Detect damages in conical shells using curvature mode shape and wavelet finite element method, Int. J. Mech. Sci., in press, http://dx.doi.org/10.1016/j.ijmecsci.2012.10.010.

[30] X. Jiang, Z.J. Ma, W.-X. Ren, Crack detection from the slope of the mode shape using complex continuous wavelet transform, Comput.-Aided Civil Infrastruct. Eng. 27 (3) (2012) 187–201.

[31] U.P. Poudel, G. Fu, J. Ye, Wavelet transformation of mode shape difference function for structural damage location identification, Earth Eng. Struct. Dyn. 36 (8) (2007) 1089–1107.

[32] M. Solís, A. Romero, P. Galvín, Monitoring the mechanical behavior of the weathervane sculpture mounted atop seville cathedral's giralda tower, Struct. Health Monit. 9 (1) (2010) 41–57.

[33] G. Strang, N. Truong, Wavelets and Filter Banks, Wellesley College Press, Cambridge, 1996.

[34] P. Abry, Ondelettes et turbulence. Multirésolutions, algorithmes de décomposition, invariance d'échelles, Diderot Editeur, Paris, 1997.

[35] T. Mathworks, Matlab, 2011.

[36] I. Daubechies, Orthonormal bases of compactly supported wavelets, Commun. Pure Appl. Math. 41 (7) (1988) 909–996.

[37] S. Mallat, A Wavelet Tour of Signal Processing, Academic Press, London, 1999.

[38] J.C. Hong, Y.Y. Kim, H.C. Lee, Y.W. Lee, Damage detection using the Lipschitz exponent estimated by the wavelet transform: applications to vibration modes of a beam, Int. J. Solids Struct. 39 (7) (2002) 1803–1816.

[39] D. Ewins, Modal Testing: Theory, Practice, and Application, Research Press Ltd., Philadelphia, USA, 2000.

[40] B. Peeters, G.D. Roeck, Reference-based stochastic subspace identification for output-only modal analysis, Mech. Syst. Signal Process. 13 (6) (1999) 855–878.

[41] R. Brincker, L. Zhang, P. Andersen, Modal identification of output-only systems using frequency domain decomposition, Smart Mater. Struct. 10 (3) (2001) 441.

[42] E. Reynders, G.D. Roeck, Reference-based combined deterministic–stochastic subspace identification for experimental and operational modal analysis, Mech. Syst. Signal Process. 22 (3) (2008) 617–637.

[43] A. Messina, Refinements of damage detection methods based on wavelet analysis of dynamical shapes, Int. J. Solids Struct. 45 (14–15) (2008) 4068–4097.

[44] A. Gentile, A. Messina, On the continuous wavelet transforms applied to discrete vibrational data for detecting open cracks in damaged beams, Int. J. Solids Struct. 40 (2) (2003) 295–315.

[45] X. Shao, C. Ma, A general approach to derivative calculation using wavelet transform, Chemometrics and Intelligent Laboratory Systems 69 (1–2) (2003) 157–165.

[46] A. Pandey, M. Biswas, M. Samman, Damage detection from changes in curvature mode shapes, J. Sound Vib. 145 (2) (1991) 321–332.

[47] R.J. Allemang, D.L. Brown, A correlation coefficient for modal vector analysis, in: Proceedings of the International Modal Analysis Conference and Exhibit, 1982, pp. 110–116.

[48] J. Xiang, M. Liang, A two-step approach to multi-damage detection for plate structures, Eng. Fract. Mech. 91 (1) (2012) 73–86.

[49] V. Pakrashi, A. O'Connor, B. Basu, A study on the effects of damage models and wavelet bases for damage identification and calibration in beams, Comput.-Aided Civil Infrastruct. Eng. 22 (8) (2007) 555–569.